PERGAMON

Carbon 41 (2003) 1127–1141

CARBON

Electrolytic, TEM and Raman studies on the production of carbon nanotubes in molten NaCl

Ian A. Kinloch, George Z. Chen, Joanne Howes, Chris Boothroyd[1], Charanjeet Singh, Derek J. Fray*, Alan H. Windle

Department of Materials Science and Metallurgy, University of Cambridge, New Museums Site, Pembroke Street, Cambridge CB2 3QZ, UK

Received 11 December 2002; received in revised form 6 January 2003; accepted 17 January 2003

Abstract

The production of carbon nanotubes (CNTs) by the electrolysis of molten NaCl was investigated by examining the effect of electrolysis duration, current density and voltage. It was found that as the electrolysis was run for longer periods the cathode eroded, changing the current density and consequently preventing nanotube production. The electrolysis was also inhibited by the anode effect and the formation of a sodium layer on the top of the electrolyte. The cell was modified to avoid these difficulties and then optimised under voltage control. Minimum and optimum voltages and current densities were found for CNT production. However, it was discovered that the percentage of nanotube produce still fell as the electrolysis progressed despite minimising the variation in the current density. The nanomaterial produced was studied by TEM. In particular, it was observed that half of the nanotubes were coated with amorphous carbon, suggesting a two-stage growth process. No link, though, was established between the growth conditions and the morphology of the nanotubes. Raman spectroscopy showed that the quality of the nanotubes was comparable to those produced by the CVD route. Titration was used to establish the uptake of sodium into the cathodes, providing evidence for the intercalation growth mechanism.

Keywords: A. Carbon nanotubes; B. Intercalation; C. Electron microscopy; Raman spectroscopy

1. Introduction

The molten salt production method for carbon nanotubes (CNTs) was discovered by Hsu et al. [1] in 1995 and since then relatively little work has been published on it, especially compared to the catalytic vapour deposition (CVD) method. The nanotubes are produced by the electrolysis of a molten halide salt using a graphite cathode and anode. During the electrolysis the cathode erodes and nanoparticles, including nanotubes, are found in the salt. The nanotubes produced are usually multi-walled, however Bai et al. have recently grown SWNTs [2]. The method is unique compared to other production methods since it occurs in the condensed phase and uses graphite as the feedstock at relatively low temperatures. (Arc-vapour and laser methods also use graphite as feedstock but ablate the graphite at high temperatures.) The method also allows the production of filled nanotubes and nanowires in a one step process by the addition of a low melting metal or salt to the electrolyte (e.g., $SnCl_2$, Sn, Pb and Bi into LiCl [3–5]). The main parameters in the electrolysis are current density, cell voltage, temperature and electrolyte composition. Unfortunately, these parameters are interdependent, making it hard to establish their effects on nanotube production.

Hsu et al. found that for a LiCl electrolyte the percentage of nanotubes in the nanomaterial produced (*purity*) varied with the current and the depth of the cathode [6]. The optimum conditions for a high purity (20–30 vol% nanotubes) were found to be a cathodic surface area of 2–2.9 cm^2 and a current of 3–7 A. Lower and higher currents were found to produce mainly amorphous carbon. Dimitrov et al. have conducted a further investigation on LiCl but used voltage rather than current control for the

*Corresponding author. Tel.: +44-1223-334-300; fax: +44-1223-335-637.

E-mail address: djf25@hermes.cam.ac.uk (D.J. Fray).

[1]Current address: IMRE, 3 Research Link, Singapore 117602, Singapore.

0008-6223/03/$ – see front matter
doi:10.1016/S0008-6223(03)00020-4

electrolysis [5]. They found that for voltages of <8.4 V, the purity of the nanotubes increased with increasing voltage. As yet the effect of the current and voltage conditions on purity has not been published for a NaCl electrolyte and is presented in this paper.

The cathodic current density (i_C) has been found to affect the degree of erosion of the cathode, with the erosion increasing with increasing i_C [6]. This erosion prevents the experiment from being run for long periods since the entire cathode can be consumed. Therefore, in order to scale up the route, Dimitrov et al. replaced the eroded material fed a long cathode into the electrolyte as the experiment progressed [5].

A different optimum temperature for nanotube production has been found for each electrolyte composition, with the purity decreasing significantly on either side of this temperature. For NaCl and LiCl electrolytes the optimum temperature was just above the melting point of the salt [7].

The electrolyte used has a large influence on the purity but, as previously discussed, so does the temperature of use. Therefore, caution has to be used in interpreting the results on the different types of electrolyte since a poor purity maybe due to the temperature as much as the electrolyte. It has been reported that using $SnCl_2$ and $ZnCl_2$ electrolytes produces no nanomaterials, whereas using KI and $CaCl_2$ electrolytes produces only amorphous carbon and encapsulated particles [6]. KCl, LiBr, LiCl and NaCl electrolytes all have produced nanotubes, with the maximum reported purities being 5, 30, 30–40 and 50 vol%, respectively. Interestingly, the electrolytes that produced the highest purities had the lowest rate of erosion of the cathode [7].

There has been no detailed work on the effect of the duration of the electrolysis. It was discovered that nanomaterial is only found in the electrolyte after the first 5–10 s of the reaction [8]. Also, long experiments (50 min) were run in a large cell by Dimitrov et al. without a noticeable difference compared to the shorter experiments [5].

There have been several proposed growth mechanisms for the molten salt electrolysis method. The authors have previously suggested that the alkali metal ions intercalate into the cathode to form a graphite intercalation compound [9]. The intercalated ions are reduced and expand the lattice of the graphite, putting strain upon it. The strain increases on the lattice as more metal is intercalated until the lattice fragments into M_xC_y particles (M=alkali metal). It is believed that in a critical range of x and y the M_xC_y particles aggregate and react to form nanotubes, possibly leaving part of the metal/carbide inside the formed nanotube. When x and y are outside this critical range other types of nanoparticles are produced. Kaptay et al. agrees with the initial intercalation stage but suggests that the fragments responsible for the nanotube formation are graphite sheets rather than M_xC_y particles [10] (i.e., $x=0$ for nanotube production). These growth mechanisms are similar to that found in the recent work on producing nanoscrolls from graphite [11]. The nanoscrolls were produced by exfoliating a graphite lattice by the forming polymer chains between the graphite planes. This result shows that the electrolytic insertion of alkali metals is not required for nanomaterial production. However, metal–carbon particles might be needed to break the carbon into species which are sufficiently small to produce a nanotube opposed to a continuously rolled scroll.

An alternative method for the growth of nanotubes is that the nanotubes are extruded directly out of the intercalated graphite lattice. Finally, it has been proposed by Hsu et al. that the metal deposits onto the cathode and forms a carbide [8]. The carbon is then extruded from the surface of this carbide as a nanonozzle to form the nanotubes.

This paper initially examines the effect of electrolysis duration on a previously used cell [7]. The erosion pattern of the cathode, the stability and repeatability of the cell and the purity and morphology of the product were investigated. Based upon these results, the cell was modified to include a ceramic sheath and by expanding the surface area of the anode. The modified cell was then optimised with respect to voltage and, through analysis, cathodic current density (i_C) to give the first study of these parameters for NaCl. Several longer experiments were run at this optimised voltage with the cathode being continually fed in to replace the eroded material. The products from all these experiments were examined using TEM and Raman. Finally, the sodium content in the cathodes was measured to provide further evidence for the intercalation growth mechanism.

2. Experimental method

2.1. Experimental set-up

The design of the first cell used is shown in Figure 1 and its parameters are given in Table 1. The cathode (6 mm diameter graphite rod, EC 4 grade from Graphite Technologies) was inserted to a depth of 10 mm in the electrolyte. The cell was run at the published conditions of 820 °C in argon at a constant current of 5 A (initial i_C of 1.1 A cm^{-2} [7]). The length of the experiments was varied from 3 min to when the cathode in the electrolyte had eroded completely (11.5 min).

The second cell (Fig. 2, Table 1) was designed to eliminate the difficulties found when using the first cell. The cathode in this second cell was surrounded by a ceramic sheath and exposed to the electrolyte at the bottom of the cell in order to minimise its exposure to the chlorine gas formed during the electrolysis [5]. The cathode was also pushed against a ceramic base plate so that it could be inserted to a known depth without any knowledge of the erosion history. (The base plate prevented the creation of chlorine gas close to the cathode.) The second cell was larger than the first cell, with a greater anodic surface area, and contained an increased amount of electrolyte.

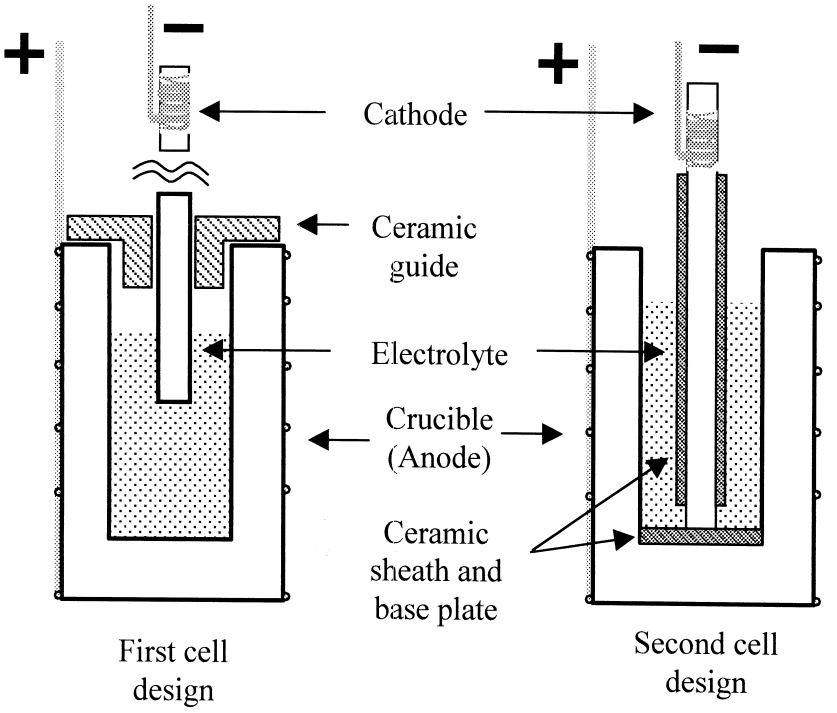

Fig. 1. The two cell designs used for the work. (The second cell was a modified version of the first.) These cells were used inside a heated reactor tube with an argon atmosphere, as described in Ref. [7]. The parameters of the cells are given in Table 1.

The second cell was run at 870 °C in argon to prevent the solidification of the electrolyte between the top of the sheath and the cathode. This solidification was due to the small size of the furnace, meaning that the top of the sheath was slightly out of the hot zone. The electrolyses were run in voltage control to give the current the freedom to adapt to changes in the cell's resistance. (It should be noted that the cell voltage, and not the potential at the cathode, was controlled. The latter would have been preferable but there was difficulty in obtaining a suitable reference electrode.) The causes of the change in the resistance of the cell were the build-up of sodium metal and carbon in the electrolyte and the erosion of the cathode. It was hoped that i_C could be stabilised by using voltage control since the current would be able to decrease as the surface area of the cathode decreased.

Table 1
Comparison of the parameters for the two cells used

Parameter	First cell	Second cell
Internal diameter of cell	20 mm	30 mm
Mass of salt used	23.4 g	48 g
Guides used	Ceramic guide at top	Cut-away ceramic sheath
Temperature	825±7 °C	860±15 °C
Initial depth of cathode	20±1 mm	10 mm
Current or voltage control	Current	Voltage
Range of controlled parameter	5A (error <2%)	3.5–9 V
Duration of electrolysis	3–11.5 min	2×10 min or 30–60 min

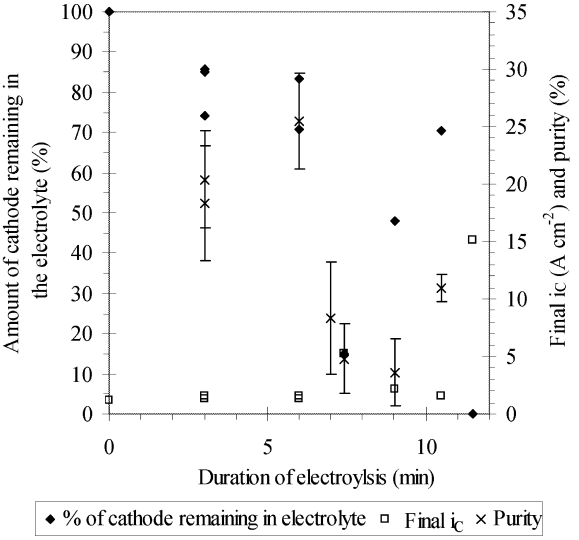

Fig. 2. The purity, i_C and amount of erosion of the cathode in the first cell as a function of electrolysis time. The cell was stable for the first ~6 min, after which the large scale fracturing of the cathode occurred.

Three sets of experiments were run in the second cell:

a) Optimisation experiments

Optimisation experiments were run at various voltages to establish the optimal conditions for nanotube growth. Two 10-min long electrolyses were run in the same electrolyte at each voltage, with a new cathode being used for each electrolysis.

b) Feeding experiments

Feeding experiments were run at the optimal voltage of 4.5 V. The cathode was inserted into the cell every 15 min during the electrolyses to replace the cathode that had eroded away. A shorter time between insertions had been considered but it was found that the current took 30 s to stabilise after each insertion. Ideally, for future experiments, the cathode would be fed in continuously and steadily (i.e., by using an appropriate weight on top of a long, graphite rod).

c) Surface renewal experiment

Finally, a surface renewal experiment was run. This experiment was identical to the feeding experiments, but the cathode was removed every 15 min and its surface filed away before it was re-inserted. (NB: The grain size was 5 μm so the filing of the cathode's surface removed a layer ~40 grains deep.) This experiment was conducted to examine the effect of a fresh surface on the nanotube purity and was done to address the differences in the purity observed between the optimisation and feeding experiments.

All these experiments used the same procedure as that described by Chen et al. [9]. Briefly, the cells were enclosed in an Inconel reaction tube and were used within an argon atmosphere at atmospheric pressure. The cell and tube were heated using a vertical furnace to initially 100 °C to dry the NaCl and then to the electrolysis temperature. The cathode was inserted into the reaction tube, allowed to reach thermal equilibrium and then inserted into the cell. After the electrolysis had been conducted the furnace was switched off and allowed to cool overnight. The electrolyte, which contained the nanomaterial produced, was dissolved in water and then the nanoparticles were collected at a toluene–water interface. Electron microscopy samples were prepared by gentle ultrasounding collected material in toluene and then placing a drop of the dispersion onto a holey carbon film supported on a 400-mesh copper grid.

2.2. Analysis of product

The nanotubes produced were examined using transmission electron microscopy (TEM) (the microscopes used were a Jeol 200CX, Jeol 4000FX and Philips CM30). The structure of the products was evaluated using a mixture of high-resolution imaging, diffraction and dark field imaging.

The purity of the nanotubes in a sample is a difficult parameter to evaluate absolutely and inevitably is dependent on the experimenter [12]. In this work the following procedure was used to measure the purity and ensure self-consistency between measurements. The measurement was based upon the fact that the nanomaterial produced was always aggregated into discrete, micron-sized aggregates on the TEM sample grid, with typically five aggregates per 63.5-μm grid square. The purity in each aggregate was estimated by eye in at least 10 grid squares. The overall purity of the sample was then taken as the mean percentage of nanotubes in each grid square and the error was taken as the error on the mean. The analysis of each sample took 2–3 h and the repeatability of the method was shown by obtaining purities of 5 ± 2 and $4\pm3\%$ for two samples taken from the same experiment.

The samples were also analysed using Raman spectroscopy (Reinshaw 1000 Ramascope, 514.5 nm wavelength laser.) This technique was mainly used to check if single-walled tubes were present in the sample and to assess the relative crystal size of the graphite in the material.

2.3. Sodium content in the cathodes

The sodium content in the cathodes was measured by using titration in order to provide evidence for the intercalation of sodium during the electrolysis. (Titration has been used previously to investigate the erosion of graphite electrodes by sodium intercalation in the Hall-Herault process [13].) This technique was chosen since it only includes the elemental sodium and Na_2O (formed by oxidation by air) and excludes any physically absorbed NaCl. Also, titration can detect lower concentrations of sodium compared to other techniques such as energy dispersive X-ray analysis. Samples were taken from the cathode, ground using a pestle and mortar and placed in either water or dilute $HCl_{(aq)}$. When water was used, 0.6 g of ground cathode was placed in 25 ml of distilled water, left for 3 weeks and then titrated against 0.01 M $HCl_{(aq)}$. When HCl was used, 0.5 g of cathode was placed in 50 ml of 0.1 M $HCl_{(aq)}$, stirred at 360 rpm for 10 days and then titrated against $NaOH_{(aq)}$. The latter procedure was taken from Liao and Øye [13]. For both methods the difference in the pH between the solvent and the solution was assumed to be entirely due to extracted Na.

3. Results and discussion

3.1. Reliability and stability

The first cell design (*current controlled*) was found to be unreliable with 20% of the experiments being

abandoned. The most common problem was the shorting between the electrodes, which occurred in the longer experiments. When the shorting occurred, the cathode did not erode and no nanomaterial was produced. The cause of the shorting was believed to be the sodium metal that was deposited at the cathode and then floated to the top of the electrolyte. The sodium layer was characterised by the bright orange flare that was observed when air was introduced into the system.

When running the cell at 5 A, there was a range of ~3 V in the starting voltages of the experiments, despite all of them using the same cell set-up and current. The voltage was approximately constant over the time frame of the experiments. However, there were occasionally jumps of >1 V in voltage which lasted a few seconds during all the experiments. In extreme cases the cell resistance had increased during these jumps such that the power supply could no longer deliver the 5 A current. The electrolysis, though, could be restarted successfully if the electrolysis was stopped for about 1 min. This increase in resistance is believed to be due to the chlorine gas that formed during the electrolysis insulating the anode and/or preventing the electrolyte from wetting the anode. The chlorine would have then dissipated upon stopping the experiment or lowering the current. This phenomenon is well known in the electrolysis of halide salts and is referred to as the anode effect [14].

The second cell (*voltage controlled*) was significantly more reliable than the first due to the sheath preventing any shorting and the enlargement of the cell eliminating the anode effect. When running under voltage control, the current was found to drop during the first 100 s of the electrolysis. The value of the current was similar for the two electrolysis runs made in the same electrolyte but for the electrolyses conducted at the same voltage but in different electrolytes the current could vary by up to 1 A. This difference in current corresponded to a variation of 0.5 A cm^{-2} in the i_C and could have a significant effect on the rate of the erosion of the cathode and the products formed as described later.

The aim of using voltage control for the second cell was to keep the i_C constant. Unfortunately, as Table 2 shows, this consistency was not always achieved when the cell voltage was ≥5.7 V. The high degree of erosion of the cathode due at the high voltages probably caused these instabilities.

3.2. Erosion of the anode

The anode was observed to pit in both cells during the electrolyses. To evaluate this erosion, the second cell was run for 20 min with a cathode made from Kanthal wire. A few milligrams of carbon were extracted from the electrolyte after the electrolysis. However, these pieces were too large to collect at the toluene–water interface and therefore were not nano-sized. This agrees with the work by Hsu et al. who argued that the nanotubes were made at the cathode [6]. (They used a metal anode and a carbon cathode and found nanotubes in the electrolyte after electrolysis.)

3.3. Erosion of the cathode

The erosion of the cathode was found to follow a typical pattern as the electrolysis progressed. The surface of the cathode was slightly roughened and then fine, sub-mil-

Table 2
The cathodic current density at 100 s and at the end of the electrolysis; the type of cracking refers to 'fine' cracks on the surface and 'coarse' millimeter-sized cracks

Exp no.	Type of experiment	Voltage (V)	i_c (A cm^{-2})						Type of cracking
			1st run in the electrolyte			2nd run in the electrolyte			
			At 100 s	At end	Difference (%)	At 100 s	At end	Difference (%)	
1	Optimisation	3.5	0.42	0.49	**15**	0.53	0.51	**−4**	Fine
2		4.5	0.95	0.82	**−14**	0.89	0.83	**−7**	Fine
3		4.5	0.75	0.71	**−5**	0.81	0.82	**1**	Fine
4		5.7	1.32	1.36	**3**	0.8	1.95	**83**	Coarse
5		7.0	1.74	2.73	**45**	1.81	2.81	**43**	Coarse
6		9	2.70	6.99	**89**	2.66	2.59	**−3**	Coarse
7	Semi-	4.5	1.08	2.33	**147**				Coarse
8	continuous feeding	4.5	0.89	1.23	**33**				Diameter thinned
9	Surface renewal	4.5	0.87	0.73	**-17**	0.88	1.15	43	Fine on first run. Coarse on the rest
			0.91	1.36	**39**	0.94	1.34	35	

For the optimisation experiments, a 'run' refers to the 10 min electrolysis conducted with each cathode. The cathode was filed three times in the surface renewal experiment; the initial insertion and first filing are on the top row and second and third filings are on the second row.

limetre cracks started to appear. These cracks expanded, growing up to 1 mm in width and penetrated the cathode. The crack growth occurred particularly at the end of the cathode whether the i_C was highest, and caused the end of the cathode to expand (for image see Ref. [9]). The cracks continued growing until they had penetrated completely through the lower edges of the cathode, causing millimetre-sized pieces of cathode to fall away into the electrolyte. At this stage the cathode had a pointed tip. The cracks then grew towards the centre of the cathode, causing more large pieces to break away and give an approximately flat end to the cathode. Crack growth proceeded in a similar manner from the newly formed end of the cathode until all the cathode in the electrolyte had been eroded.

Fig. 2 shows the amount of erosion of the cathode as a function of electrolysis time for the initial cell running at 5 A. The erosion for the initial 6 min of the electrolysis was found to be stable and repeatable. However, the rate of erosion after this time increased greatly and became unpredictable due to the fracturing of millimetre-sized pieces of cathode.

The optimisation experiments conducted with the second cell showed that the rate of erosion increased with increasing cell voltage, as found by Hsu et al. in LiCl [6]. For the experiments conducted at voltages $\leq$4.5 V, only fine cracking occurred on the cathode. This cracking was similar to that found on the initial cell's cathodes for short periods of time. In contrast, for the experiments at $\geq$5.7 V, coarse cracking occurred, with large pieces of cathode breaking off and the cathode expanding. At 9 V the cracking became audible.

One of the feeding experiments (Exp. 8) ran at 4.5 V, however, did not fit into the above trends. In this experiment the fine cracking slowly progressed to give a gradual thinning of the cathode with no large cracks being observed (Fig. 3). This was an extension of the fine cracking seen in the optimisation experiments and was desirable since it kept i_C relatively constant. (It is plausible that the alkali ions were driven into the cathode's lattice at a sufficiently fast rate to fracture the top of the surface but slow enough not to cause the deep cracks.) However, when the experiment was repeated, the gradual erosion did not occur (Exp. 7). Analysis of the data showed that this change was due to the difference in the starting i_C between the experiments (Table 2). Further analysis of the table showed that when i_C was $<\sim$1 A cm^{-2} only gradual erosion and fine cracking occurred, and at higher i_C the erosion progressed to large cracks and fracture.

The dependence of the rate of the erosion on i_C was a major problem for controlling the growth conditions of the cell since it caused positive feedback; as the cathode eroded, i_C increased which in turn accelerated the erosion of the cathode. (The shape of the erosion graph in Fig. 2 shows the effect of a feedback mechanism.) Therefore, for future work, it is preferable to keep i_C constant by either minimising the erosion by using a low i_C ($<$1 A cm^{-2}) or by continuously feeding the cathode into the cell to replace the eroded material. Also, the experiments should be run in current control to ensure that the desired initial i_C is obtained.

3.4. Factors affecting the nanotube purity

3.4.1. Temperature and cell design

The first cell produced nanotubes in purities of up to 25% at 820 °C but produced only carbon sheets and no nanotubes at 870 °C. The second cell, though, was run at 870 °C throughout and produced nanotubes in purities of up to 25% under similar current densities and voltages to those used for the first cell. Therefore, while a temperature dependence was found, fitting in with the work of Chen et al., the actual dependence was found to vary with the design of the cell [7]. This result was unexpected and has

Fig. 3. An optical micrograph of the cathode from experiment 8. Notice how the cathode thins towards the right hand side, where it was exposed to the electrolyte.

implications for future work since new cell designs will need their operating temperature optimised.

3.4.2. First cell: effect of electrolysis duration and current density

In the first cell, the purity of the nanotubes was found to be constant for the first 6 min (Fig. 2). However, after this time the purity decreased and the data became scattered. This transition occurred at the same time as when the large pieces of cathode started to break away. Previous work has found that i_C affects purity in other electrolytes [5,9]. Therefore the purity drop was probably due to the i_C increase caused by the erosion of the cathode.

3.4.3. Second cell: effect of voltage, current density and charge passed

No nanotubes were produced at 3.5 V and the highest purity of nanotubes (25%) was produced at 4.5 V (Fig. 4). Therefore, there is a minimum and optimum voltage for nanotube production. The purity fell as the voltage was increased beyond 4.5 V, such that at 9 V virtually no nanotubes were produced although the cathode erosion always occurred. The experimental data were replotted in terms of i_C by representing the data points as rectangles, with the width showing the possible values for i_C during the experiment and the length giving the experimental error in the purity analysis (Fig. 5). The i_C value range was taken from the current at 100 s divided by the initial surface area and the highest current divided by the 'final geometric' surface area. (BET studies could be used in future to determine the actual surface area. However, the majority of the geometric changes observed were sufficiently large to negate the effect of the cracking.) As Fig. 5 shows, there was a minimum i_C and optimal i_C between 0.7 and 1.1 A cm^{-2}, with the purity falling as the i_C further increased.

The minimal and optimal values of i_C and cell voltage for nanotube production are further apart for the NaCl electrolyte than for the LiCl electrolyte [5]. This difference can be explained by the intercalation growth mechanism, the difference in the alkali atoms' sizes (Na=1.90 Å, Li=1.55 Å) and the fact that at higher current densities more ions will intercalate [15]. There will be an optimum intercalation and erosion rate for which the right fragments for nanotube formation will be produced. A larger metal atom will expand the lattice more efficiently than a smaller metal atom and therefore it will require a lower current density to fracture the cathode.

The feeding experiments produced nanotubes in purities approximately half of that found in the optimisation experiments run at the same voltage (Fig. 5). The low purity in one of the experiments (Exp. 7) was due to its initial high i_C causing heavy cracking of the cathode. However, the other experiment (Exp. 8) had similar i_C values to the optimisation runs but still the purity was lower. Therefore, a factor other than i_C had to be the cause. One possibility was that the intercalation (or reaction) sites on the cathode had become exhausted [16]. (The exhaustion would not have been observed by Dimitrov et al. since their cathodes fractured so new surfaces were always being formed [5].) The surface renewal experiment was run to check this hypothesis where instead of pushing the cathode into the cell every 15 min, the top layer of the cathode was filed away. However, this filing did not increase the purity

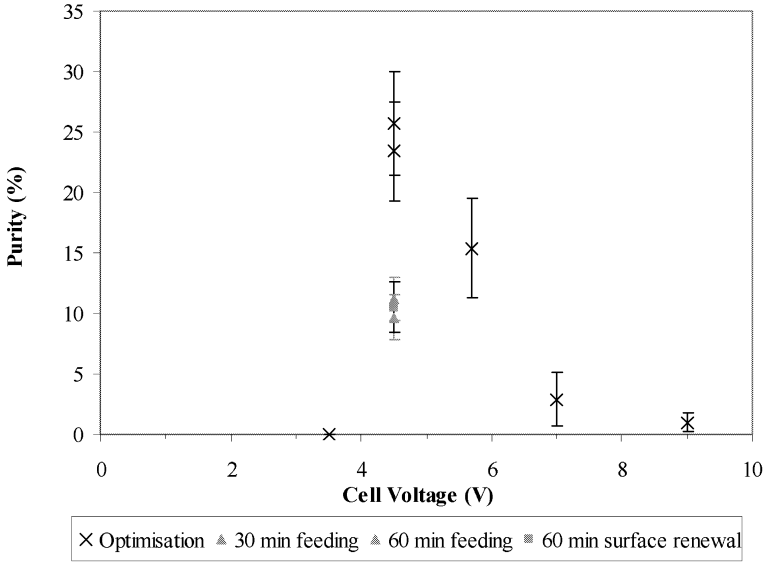

Fig. 4. The purity versus cell voltage for the second cell. The graph shows that there is both a minimal and optimal voltage for nanotube growth. NB: There is a point on the graph at 3.5 V, 0%.

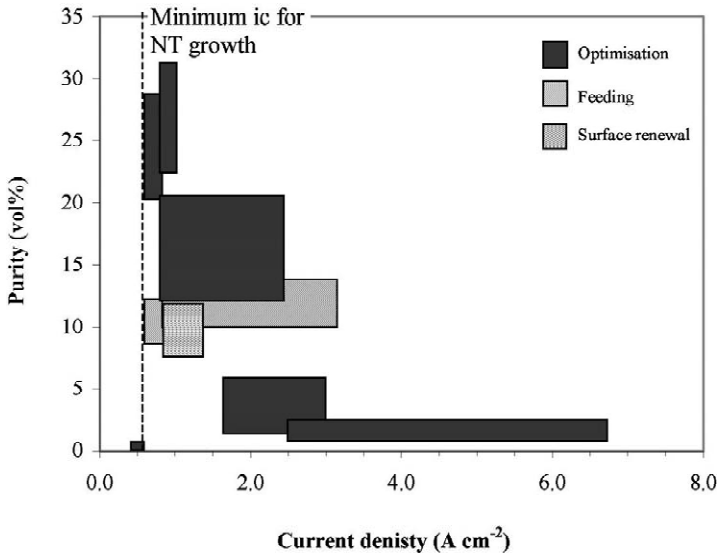

Fig. 5. The purity data from the second cell plotted as a function of cathodic current density (i_C). The length of the rectangles represents the possible variation in current density during the experiment and the height of the rectangles gives the purity and its experimental error.

so the exhaustion of the intercalation sites was not the problem.

Another possible cause of the decrease in purity was that the salt had become saturated with sodium in the longer experiments due to the amount of electrolyte consumed. This excess sodium could have reacted with the M_xC_y species, preventing nanotube formation or coated the cathode surface, even when a fresh surface was placed in the electrolyte. If the amount of electrolyte consumed was the problem, then the optimisation experiments have to be considered in terms of either voltage or i_C and charge passed. Fig. 6 shows this assumption can be justified. However, the stability of the purity in the first cell, in the initial 6 min, suggests that a minimum percentage of electrolyte has to be consumed before there is an effect.

3.5. Mass of nanomaterial produced

The mass of the collected amount of nanomaterial from the second cell increased with experimental duration and i_C. The data are plotted in Fig. 7, with the data being split at an average i_C of <1.2 and >1.8 A cm^{-2}. The data was separated at this point because it corresponded to the boundary between the heavy and more gentle erosion. The

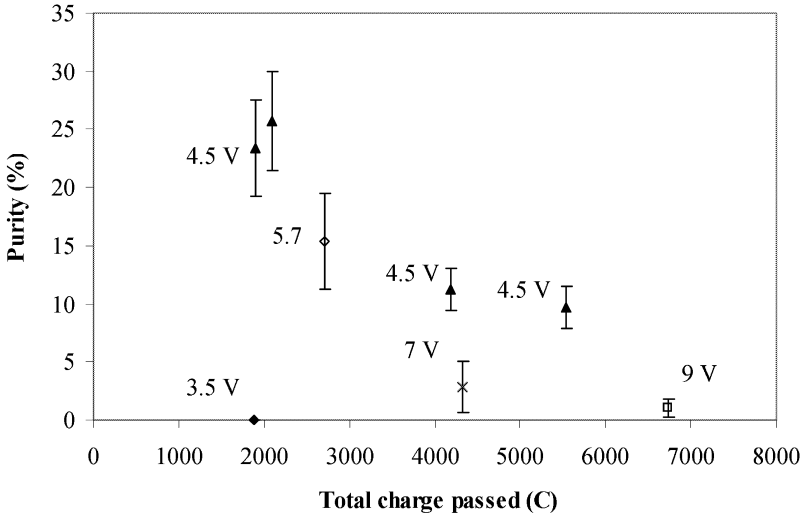

Fig. 6. The effect of the total charge passed and voltage on the purity found for the experiments run in the second cell.

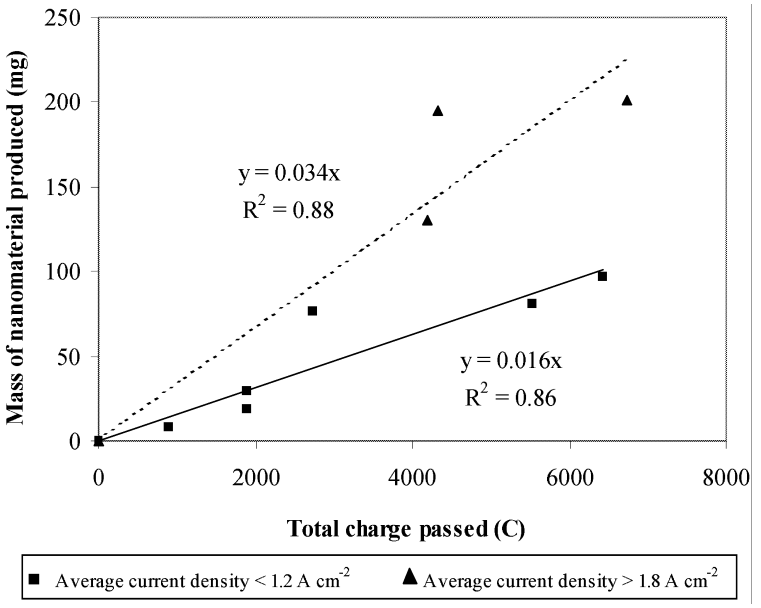

Fig. 7. The mass of nanomaterial produced as a function of charge passed and i_C for the experiments run in the second cell.

data show that the longer experiments continued to produce nanomaterial, suggesting that the fall in purity with charge passed was due to a reduction in the selectivity of the production process towards nanotubes. (i.e., initially nanotubes are produced in high purities but as the reaction progresses, different forms of nanocarbon other than nanotubes are produced, lowering the purity).

3.6. Sodium uptake in the cathodes

No sodium was found within the as-received graphite rods and the regions of the used cathodes that had not been in the electrolyte. However, the sodium was found in the regions of the used cathodes that had been in the electrolyte (Table 3). The highest measured content of the sodium was in a sample that included the material taken from the surface of the cathode. This result (4 wt%) was ~20 times higher than the other results. The anomaly could have been due to either the $HCl_{(aq)}$ being a more effective solvent than water, or the sodium in that sample being located at the surface. The latter seems more probable since the sample from the cathode's core contained less sodium than the other samples. Also, water has been effectively used as a solvent in other work [17]. Excluding this result the average sodium content the samples was 0.15 wt%.

In the literature, the uptake of sodium varies with the type of carbon. In general the uptake is less for carbon treated at high temperatures. This makes direct comparison of the sodium content with other work difficult, especially

Table 3
The sodium content found by titration in the cathodes

Solvent used to remove Na	Conditions of the electrolysis		Did the sample include the surface layer?	wt% Na	
	Current (A)	Duration (min)		Average	Error
H_2O	5	3	Yes	0.15	0.01
H_2O	5	3	Yes	0.19	0.01
H_2O	5	3	Yes	Too small to measure	
$HCl_{(aq)}$	5	6	Yes	4.04	1.2
			No	0.05	0.02
H_2O	~7	10	No	0.21	0.01

The above results were for the ends of the cathodes that were immersed in the electrolyte. The sections of these cathodes that had not been in the electrolyte were found to contain no sodium.

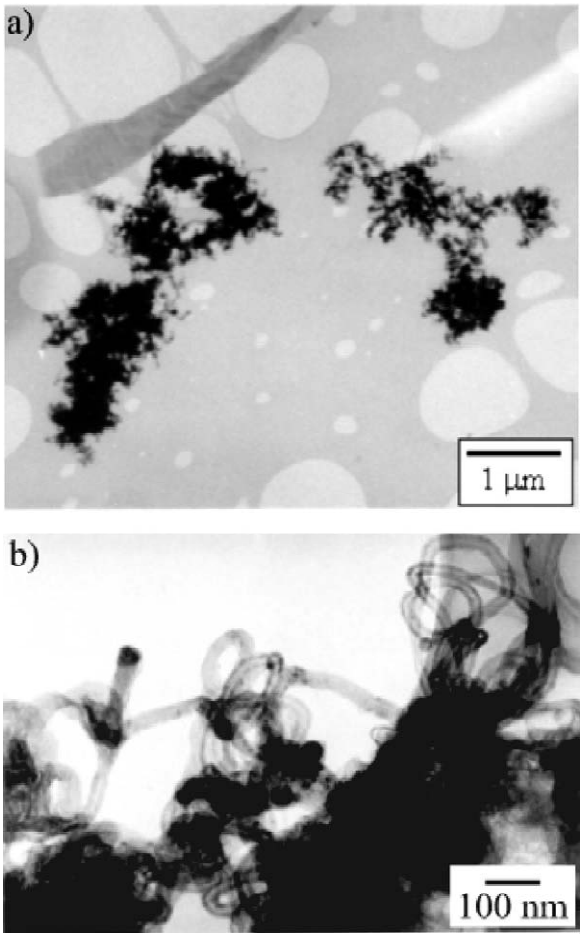

Fig. 8. TEM micrographs of (a) the typical aggregates produced and (b) a typical region of nanotubes.

as sodium can be inserted by other methods such as sodium vapour. However, the results in Table 3 are similar to the range reported by Joncourt et al. [17] and Liao and Øye [13] of 0.2–5 wt%. (The 0.2 wt% uptake was measured for carbon closest in structure to that used in this paper and the 3 wt% was inserted using the method closest to that used in this paper.)

3.7. Characterisation of product

3.7.1. TEM

The material produced contained a wide variety of types and sizes of nanoparticles and nanotubes. The material was found to be aggregated with the aggregates always containing nanoparticles but not necessarily nanotubes (Figs. 8 and 9). The nanotubes were highly entwined, similar to nanotubes produced catalytically using a floating catalyst. The nanotubes could stretch between two separate aggregates, with an end in each, but typically most nanotubes started and ended in the same aggregate with only a small section of the nanotube curving out of the aggregate. The properties of the nanotube (e.g., diameter) tended to vary within any given aggregate. The only exception to this was that nanotubes with thick surface coatings tended to cluster together. It is therefore, unclear if the aggregates were formed during the electrolysis, with the nanotubes growing together entwined, or were formed as the electrolyte solidified after the electrolysis. (It is unlikely that the aggregates were formed during the TEM sample preparation since the preparation method has been used on catalytically grown material to give well dispersed nanotubes.)

The purity of the nanotubes was found to vary (0–25 vol%) with the electrolysis conditions used, as discussed earlier. However, the growth conditions did not have an

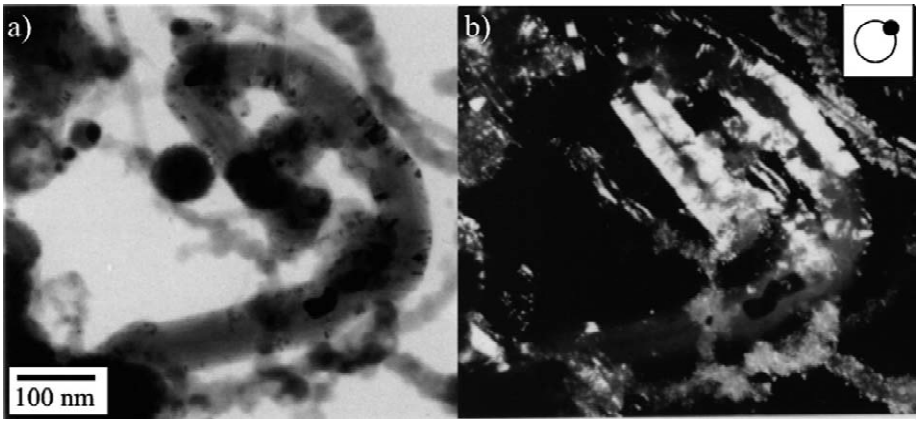

Fig. 9. Bright field (a), dark field (b) images of a typical region of nanotubes. The insert shows the relative position of the objective aperture on the 002 diffraction ring. Encapsulated material can be seen in the large nanotube and the particle.

effect on what other types of material were produced. The inner diameter of the nanotubes was 8±5 nm and the outer diameter was 22±12 nm. Despite detailed measurements, no relationship between the growth conditions and the diameters of the nanotubes could be found.

Approximately half of the nanotubes produced had clean, well-defined, outer surfaces (Fig. 8) while the rest of the nanotubes were coated with a carbon film. For 10–30% of the coated nanotubes, the film was a thick carbon layer that completely covered, or overgrew, the nanotubes (Fig. 10). The overgrowth was 45±20 nm thick, with the largest found at 120 nm. The overgrowth made it difficult to distinguish between nanotubes and solid fibres, with the most recognisable feature being the hollow running down the centre of the nanotubes. When viewed at high resolution, the overgrowth was found to contain graphitic sections but had no well-defined structure (Fig. 10a). While this overgrowth has not been previously reported for the

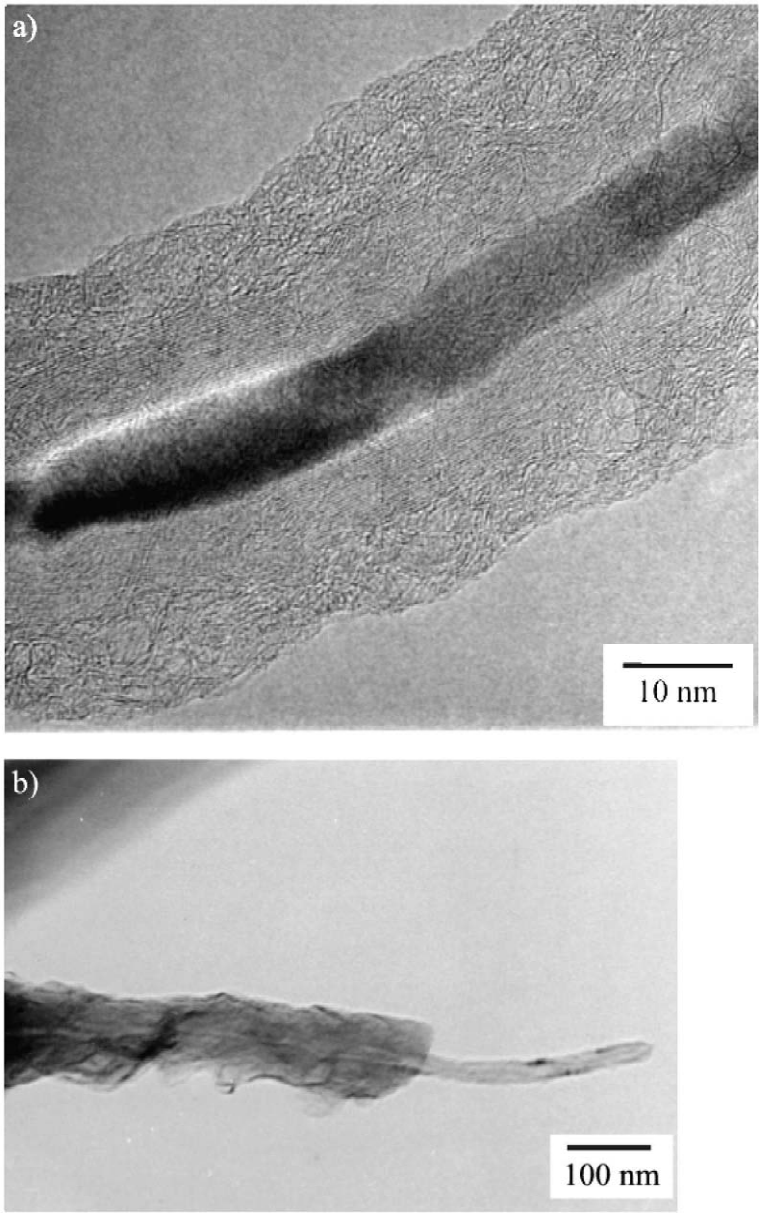

Fig. 10. Micrographs of the coating and overgrowth found on the carbon nanotubes. (a) A high-resolution image of a filled nanotube. The coating can be seen outside the lattice fringes from the well-ordered graphite walls. (b) An unusual image where the overgrowth does not fully encapsulate the nanotubes.

electrochemical production route, it is well known in the CVD route when nanotubes are grown in sooting conditions. The overgrowth has implications for the growth mechanism since it implies at least a two-stage growth, with a thickening mechanism providing the overgrowth. The overgrowth also has implications for the applications of the nanotubes. In particular, the overgrowth increases the surface area making the nanotubes more suitable for use as electrodes.

About 5% of the nanotubes viewed contained encapsulated material (e.g., Fig. 10a). This was a lower percentage than that observed with LiCl (10–40%) [7]. The material inside the nanotubes is believed to be sodium or sodium carbide, based upon past work on LiCl produced nanotubes [6,9]. Also, a few encapsulated particles were found in the electrolyte (for example the particle in the middle of Fig. 9a). Energy dispersive X-ray analysis (EDX) found that the encapsulated particles were mainly iron with some nickel and chromium. These metal particles were probably due to corroded metal from the Inconel reaction tube entering the electrolyte. The corroded metals would have then attracted any carbon in the electrolyte and upon cooling formed encapsulated particles as in the CVD production method.

A previously unreported feature of the products was solid fibres ~30 nm in diameter (Fig. 11). High-resolution imaging found that some of these fibres consisted of fused chains of nanoparticles, held together by a similar coating to that on the nanotubes (Fig. 11b). Some of the fibres observed, though, were made from very poorly formed graphite/amorphous carbon. The structure was confirmed by the little variation in contrast being observed in dark field images taken around the 002 and 101 reflections.

The other materials produced included nanoparticles, carbon sheets and tambourines (for images see Ref. [7]). The nanoparticles were the most common impurity in the samples and were approximately 50 nm in diameter. The carbon sheet consisted of crumpled carbon layers and graphitic sheets. Chen et al. have previously reported the formation of tambourines and it is possible that these tambourines are the same structure as the nano-tori viewed by AFM by Miklósi et al. [18].

3.7.2. Raman spectroscopy

The material produced gave Raman spectrum typical for multi-walled carbon nanotubes and graphitic particles (Fig. 12). All the spectra obtained had a G peak at ~1585 cm^{-1} from the in-plane vibrations of the C–C bonds and a D peak at ~1350 cm^{-1} due to the disorder in the crystals. The spectra also confirmed the TEM analysis that there was no single-walled nanotubes present in the samples. (The high curvature in single-walled nanotubes causes the G band to split at 1570 and 1590 cm^{-1} and also the radial oscillation of the nanotubes' walls produces radial breathing modes at <300 cm^{-1} [19].) The ratio of the intensities of the G and D bands (I_G and I_D) gives an indication of the crystal size within the sample, with a smaller I_D/I_G indicating a larger crystal [20,21]. For the samples grown in the molten NaCl the average I_D/I_G was 0.7, compared to 0.04 found for arc-grown nanotubes and 1.2 for catalytically grown nanotubes. No relationship was found between the purity of the nanotubes produced in NaCl and Raman spectra from the material (including I_D/I_G ratio). This result was expected since the graphitic impurities within the sample gave similar spectra to that of the nanotubes.

4. Growth mechanism

The titration of the cathodes confirmed that sodium does enter the cathode and penetrates beneath the surface. This result, combined with the literature on sodium intercalation eroding the carbon cathodes in the Hall-Heroult process [22], the effect of i_C on the rate of erosion and analogies to the nanoscroll work [11] suggests strongly that the erosion of the cathode is due to sodium intercalation. This intercalation process must also be the first stage of nanotube growth given that nanotubes are produced only when a graphite cathode erodes. The present work therefore provides further evidence supporting the first stage of the mechanisms proposed by the authors. However, it does not give sufficient evidence to decide which of the post intercalation mechanisms is correct since all these mechanisms could explain the types of nanoparticles observed. The overcoating of the nanotubes, though, does suggest a two-stage growth where the well-defined walls are formed by one process and then a second process deposits the poorly formed graphitic coating. This second process must be relatively fast since the coatings do not get thicker with experimental duration. (There is the possibility that the nanotubes lengthen with time but this is impossible to observe due to the aggregation of the material.)

5. Conclusions

The production of carbon nanotubes by the electrolysis of NaCl was studied. The pattern of the erosion of the cathode was established by running the first cell for varying periods of time. It was found that the growth conditions were stable for the first ~6 min after which the crack propagation was sufficient to cause millimetre-sized pieces of graphite to fracture from the cathode. This fracturing caused unpredictable jumps in i_C, which in turn lowered the purity of the nanotubes. The first cell was also found to be unreliable over long experimental durations due to the anode effect and shorting through a sodium layer. These problems, though, were eliminated by using a second, modified cell.

The second cell was optimised; a threshold and an optimum i_C values for nanotube production were found

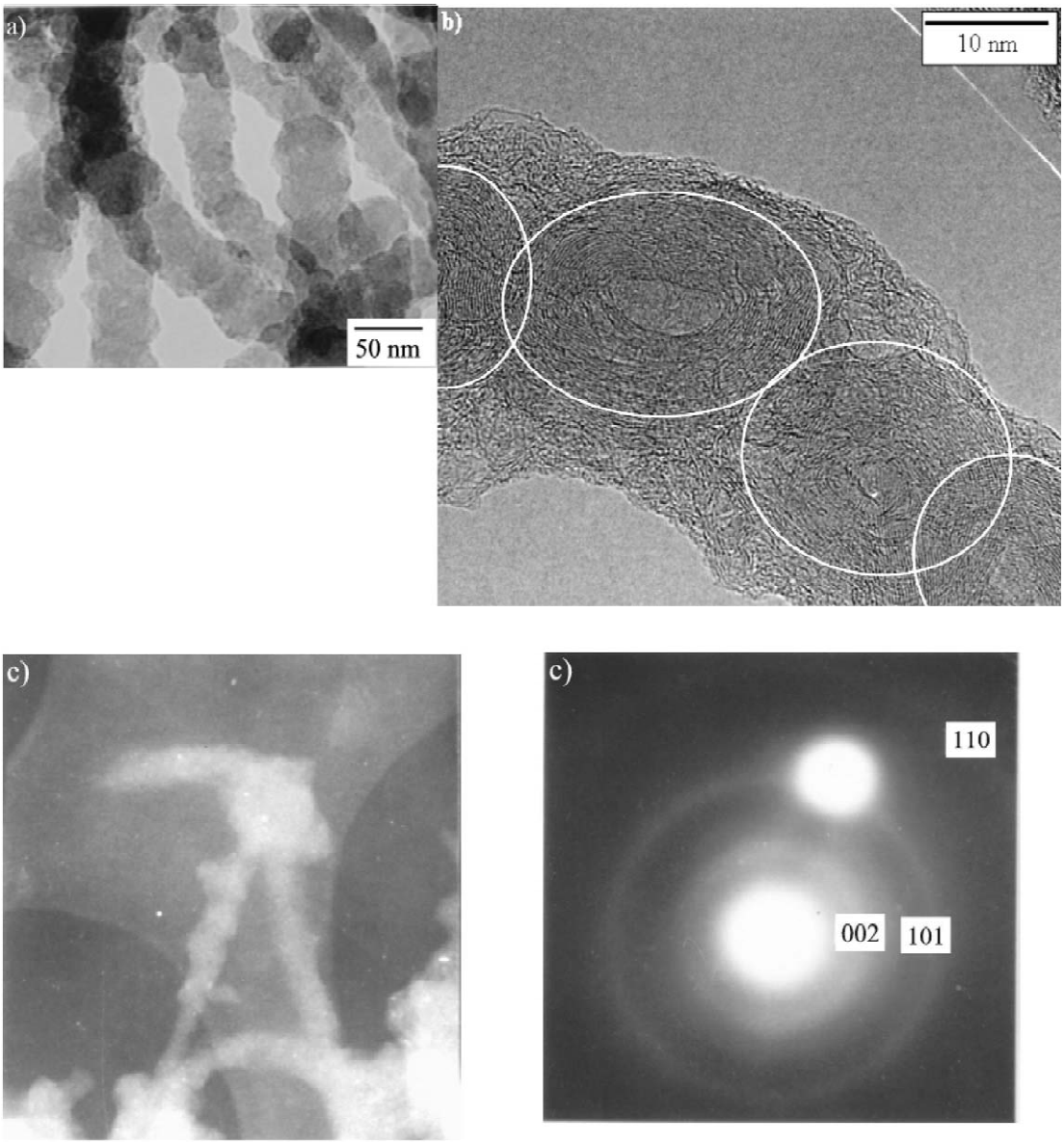

Fig. 11. Micrographs of the two types of carbon nanofibres that were produced; fused nanparticle chains (b, with the particles highlighted in white) and amorphous carbon fibres (c,d). (Micrograph c is from a set of dark field images taken from the 002 and 101 ring shown in the diffraction pattern (d). There was no variation in contrast between all these dark field images.).

between 0.7 and 1.1 A cm^{-2}. These conditions were very close together, unlike those found with a LiCl electrolyte. In the case of NaCl, the purity fell as $i_C$was increased beyond 1.1 A cm^{-2}. Also, the scale and rate of the erosion of the cathode increased with increasing i_C,with no coarse erosion occurring at low i_C (<~1 A cm^{-2}). Longer experiments were run in the second cell with the cathodes being fed into the cell at regular intervals. These experiments yielded purities lower than the shorter experiments run at a similar i_C, suggesting that the selectivity of the reaction towards nanotube growth decreased as the electrolysis progressed. (i.e., purity is also a function of total charge passed, if enough electrolyte is consumed.) It was shown that this reduction in selectivity was not due to the exhaustion of reactive sites on the cathode. A possible cause for the apparent reduction in selectivity could be the build up of excess sodium in the electrolyte. The second cell also had a different temperature dependency on purity compared to the first cell. Therefore future cell designs will need to be re-optimised with respect to temperature and

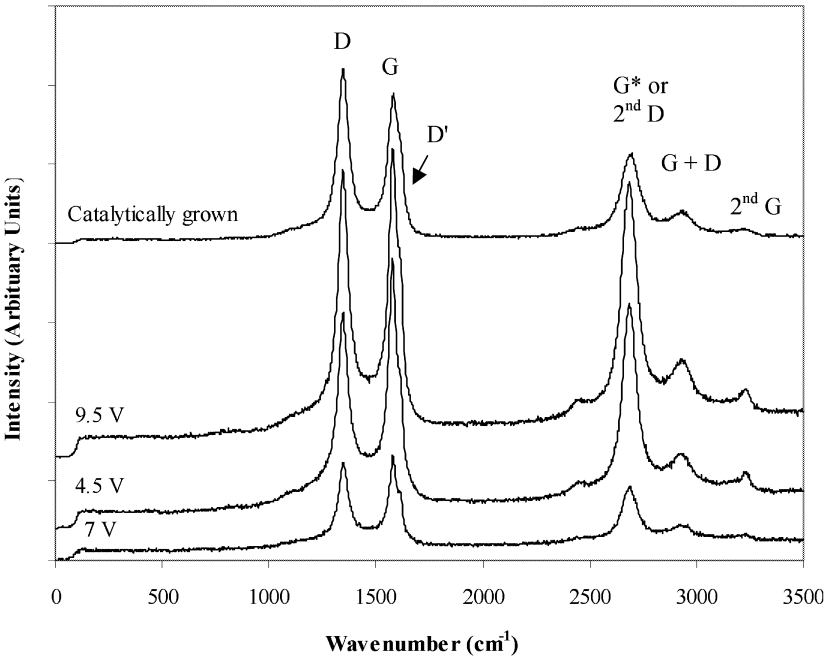

Fig. 12. Typical Raman spectra collected from the optimisation experiments run at the voltages given. No significant difference was found between the spectra obtained from the material grown at different conditions. Also shown is a spectra collected from material produced by the CVD method (Hyperion Catalysis International, >95% nanotubes, remainder catalyst).

have either continually replacement and removal of electrolyte or sufficient electrolyte to prevent saturation effects.

The material produced was examined using TEM and Raman spectroscopy. The nanotubes were found to be similar to those produced by the floating catalyst method. A significant amount of the nanotubes had an overgrowth of poorly ordered graphite. No dependency was established between the morphologies of the nanotubes (including diameter) and the growth conditions. Nanofibres were also produced, which consisted of either fused nanoparticles or amorphous carbon.

Titration was used to show that sodium had intercalated into the regions of the cathodes that were submerged in the electrolyte. This result combined with the dependences described above showed that the intercalation of the alkali metal in the cathode and the subsequent cathodic erosion is the first step of the growth mechanism. Unfortunately, it not yet possible to determine whether the subsequently formed M_xC_y species or fragmented graphite sheets are responsible for nanotube growth.

Acknowledgements

IAK is grateful to the EPSRC and BP Amoco for funding the research. GCZ thanks Darwin College Cambridge for the 2000 Schlumberger Interdisciplinary Research Fellowship.

References

[1] Hsu WK, Hare JP, Terrones M, Kroto HW, Walton DRM, Harris PJH. Condensed phase nanotubes. Nature 1995;377(6551):687.

[2] Bai JB, Hamon AL, Marraud A, Jouffrey B, Zymla V. Synthesis of SWNTs and MWNTs by a molten salt (NaCl) method. Chem Phys Lett 2002;365(1-2):184–8.

[3] Hsu WK, Li J, Terrones H, Terrones M, Grobert N, Zhu YQ, Trasobares S, Hare JP, Pickett CJ, Kroto HW, Walton DRM. Electrochemical production of low-melting metal nanowires. Chem Phys Lett 1999;301(1-2):159–66.

[4] Hsu WK, Trasobares S, Terrones H, Terrones M, Grobert N, Zhu YQ, Li WZ, Escudero R, Hare JP, Kroto HW, Walton DRM. Electrolytic formation of carbon-sheathed mixed Sn-Pb nanowires. Chem Mater 1999;11(7):1747–51.

[5] Dimitrov AT, Chen GZ, Kinloch IA, Fray DJ. A feasibility study of scaling-up the electrolytic production of carbon nanotubes in molten salts. Electrochim Acta 2002;48:91–102.

[6] Hsu WK, Terrones M, Hare JP, Terrones H, Kroto HW, Walton DRM. Electrolytic formation of carbon nanostructures. Chem Phys Lett 1996;262(1/2):161–6.

[7] Chen GZ, Fan X, Luget A, Shaffer MSP, Fray DJ, Windle AH. Electrolytic conversion of graphite to carbon nanotubes in molten salts. J Electroanal Chem 1998;446(1-2):1–6.

[8] Hsu WK, Pickett CJ, Zhu YQ, Terrones M, Grobert N, Terrones H, Hare JP, Kroto HW, Walton DRM. In: Poster presentation. Nanotec 99, University of Sussex, Sussex, UK, 1999.

[9] Chen GZ, Kinloch I, Shaffer MSP, Fray DJ, Windle AH. Electrochemical investigation of the formation of carbon nanotubes in molten salts. High Temp Mater Processes 1998;2(4):459–69.
[10] Kaptay G, Sytchev I, Miklósi J, Nagy P, Póczik P, Papp K, Kálmán X. Electrochemical synthesis of carbon nanotubes and microtubes from molten salts. In: Conference Proceedings, Euchemm 2000, 2000.
[11] Shioyama H, Akita T. A new route to carbon nanotubes. Carbon 2002;41:179–98.
[12] Duesberg GS, Muster J, Byrne HJ, Roth S, Burghard M. Towards processing of carbon nanotube for technical applications. Appl Phys A 1999;69(3):269–74.
[13] Liao X, Øye HA. Increased sodium expansion in cryolite-based alumina slurries. In: Light Metals, 127th TMS Annual Meeting of TMS Aluminium Committee, San Antonio, Texas, US, 1998, pp. 659–66.
[14] Grjotheim K, Krohn C, Malinovský M, Matiašovoský K, Thonstad J. In: Aluminium electrolysis: the chemistry of the Hall-Héroult process, Düsseldorf: Aluminium-Verlag GmbH, 1977.
[15] Mahan BH. In: University Chemistry, Reading, MA: Addison-Wesley, 1965.
[16] Xu Q, Schwandt C, Chen GZ, Fray DJ. Electrochemical investigation of lithium intercalation into graphite from molten lithium chloride. J Electroanal Chem 2002;530(1-2):16–22.
[17] Joncourt L, Mermoux M, Touzain PH, Bonnetain L, Dumas D, Allard B. Sodium reactivity with carbon. J Phys Chem Solids 1996;57(6-8):887–92.
[18] Miklósi J, Póczik P, Sytchev I, Papp K, Kaptay G, Nagy P, Kálmán ESPM. investigation of electrochemically produced carbon nanotubes. Appl Phys A 2000;71:1–4.
[19] Rao AM, Richter E, Bandow S, Chase B, Eklund PC, Williams KA, Fang S, Subbaswamy KR, Menon M, Thess A, Smalley RE, Dresselhaus G, Dresselhaus MS. Diameter-selective Raman scattering from vibrational modes in carbon nanotubes. Science 1997;275(5297):187–91.
[20] Endo M, Nishimura K, Kim YA, Hakamada K, Matushita T, Dresselhaus MS, Dresselhaus G. Raman spectroscopic characterization of submicron vapor-grown carbon fibers and carbon nanofibers obtained by pyrolyzing hydrocarbons. J Mater Res 1999;14(12):4474–7.
[21] Tan PH, Zhang SL, Yue KT, Huang FM, Shi ZJ, Zhou XH, Gu ZN. Comparative Raman study of carbon nanotubes prepared by dc arc discharge and catalytic methods. J Raman Spectrosc 1997;28(5):369–72.
[22] Sørlie M Øye HA. In: Cathodes in aluminium electrolysis, 2nd edition, Düsseldorf: Aluminium-Verlag GmbH, 1994.